DALTON
FULL PAPER

Supramolecular motifs in s-block metal bound sulfonated monoazo dyes

Alan R. Kennedy,*[a] Mhairi P. Hughes,[a] Maureen L. Monaghan,[a] Edward Staunton,[a] Simon J. Teat[b] and W. Ewen Smith[a]

[a] *Department of Pure & Applied Chemistry, University of Strathclyde, Glasgow, Scotland, G1 1XL. E-mail: a.r.kennedy@strath.ac.uk*
[b] *CCLRC Daresbury Laboratory, Warrington, England, WA4 4AD*

Received 6th March 2001, Accepted 22nd May 2001
First published as an Advance Article on the web 28th June 2001

The solid-state structures of sodium and calcium complexes of the simple sulfonated azo dyes ($[O_3SC_6H_4$-$NNC_6H_3RR']^-$ R = H, R′ = OH or NH_2; R = OH, R′ = OH) form a series of supramolecular arrays, with one-, two- and three-dimensional structural motifs and with inorganic coordination networks supporting organic channels. The dominant inorganic networks are formed *via* coordination to sulfonate groups, water molecules and the amine units, whilst the available hydroxyl groups form only hydrogen-bonds. The nature of the networks is dependent on the metal ion used with sodium ions forming close linked sheets, chains and cages reminiscent of many inorganic minerals whilst the calcium ions adopt ring-ladder structures comparable to those found in s-block amide chemistry.

Introduction

Although much recent work has been published on the role of transition metals as supramolecular building blocks,[1] little attention has been given to the comparable role of s-block metals in forming coordination networks.[2] This omission is of particular relevance to our understanding of structure–property relationships in an extensive class of solid-state colourants, which includes pigments and ink jet dyes, and is vital to the rational design of new systems in this class. As pigments and ink jet dyes are used in the form of crystals or solids in or on the media to be coloured, their physical properties depend not only upon their molecular structure but also crucially upon their solid-state structures. For example, although the nature of the chromophore in a monoazo colourant is governed by the delocalised π-system around the azo group and by the electronic nature of any substituents, it is subtly but critically altered by intermolecular interactions such as hydrogen-bonding and π-stacking. With ink jet dyes, the nature of the intermolecular interactions is also critical to surface adhesion and drying. Furthermore, the crystal structure influences the stability of a pigment to solvent, heat and light and also determines the crystal morphology which is in turn related to hiding power, stability, flow and dispersion properties.[3]

As a good pigment is by design highly insoluble (a feature shared by many polymeric, inorganic coordination arrays), it is difficult to grow the relatively large, high quality crystals needed for conventional X-ray diffraction methods, and thus little detailed structural information is available. We recently used synchrotron radiation to determine the first known crystal structure of a red azo lake pigment[4]—a representative of a commercially important class of print colourant—and showed that it had a highly anisotropic supramolecular structure featuring the classic self-assembly motifs of ligands bridging metal atoms, polydentate chelating ligands, hydrogen-bonding and π-stacking. This work indicated that azo dyes formed well ordered one-, two- and three-dimensional coordination polymers.

The work reported herein details the synthesis and structural determination of a range of more soluble azo compounds, chosen to reveal for the first time the nature of these supramolecular assemblies. A survey of the available data in the Cambridge Structural Database[5] shows that there is a lack of structural information on similar compounds. There are few studies on supramolecular motifs in sulfonated monoazos,[6] considering the widespread use of the RSO_3^- group as a solublising group in pigment chemistry and as a detoxifying agent in general.[7] One such study is especially relevant, in as far as it investigates anti-HIV active sulfonated monoazo dyes and their interactions with amino acids.[8] As noted above s-block metal coordination networks have been little studied and there is a dearth of information where these two fields (s-block metals and sulfonated azo dyes) overlap.

The ligands chosen for study are shown in Scheme 1. All have complexing groups at either end of an essentially linear molecule. The details of their solution and solid-state structures have been of interest to the colourants industry for some time[9,10] both in their own right and as useful model compounds for more complex systems. The ligands were expected to complex to the s-block metal ions Na^+ and Ca^{2+} with different bonding modes and strengths and one feature of the study was to assess the relative structural influence of interactions within the expected organic channels against the influence of interactions amongst the polar groups, including the metal ions. Another feature is the presence of an OH group *ortho* to the azo in **L′**. As well as providing an extra potential hydrogen-bonding or metal-complexing site this is also positioned so as to interact intramolecularly with the azo group and thus give a good

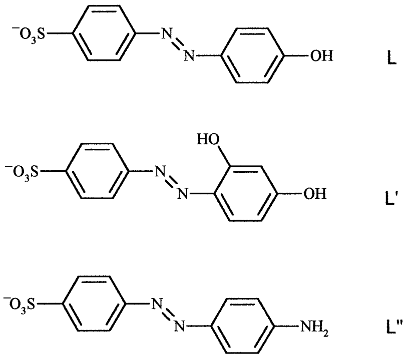

Scheme 1

DOI: 10.1039/b102106k

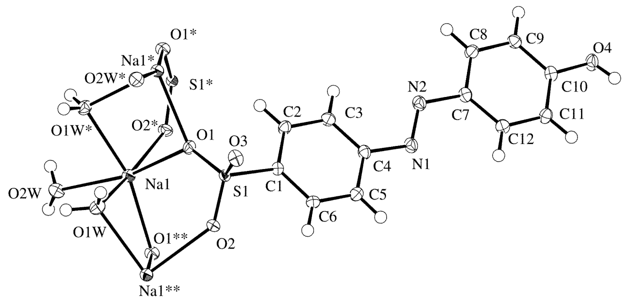

Fig. 1 The molecular structure of **NaL**. Selected bond lengths (Å); Na1–O1** 2.356(2), Na1–O2* 2.382(2), Na1–O1W* 2.386(2), Na1–O1 2.400(2), Na1–O2W 2.401(2), Na1–O1W 2.436(2) where * is $-x + 1.5$, $y + 0.5$, z and ** is $-x + 1.5$, $y - 0.5$, z.

comparison with **L**. The compounds have been investigated primarily by single crystal diffraction, using the extra intensity of synchrotron radiation where small sample size and inherent anisotropic habit made this necessary.

Results and discussion

Sample preparation

The sodium salts of **L** (4-(4′-hydroxyphenylazo)benzene sulfonic acid) and **L**′ (4-(2′,4′-dihydroxyphenylazo)benzenesulfonic acid) were prepared *via* an azide salt by standard coupling techniques.[11] The sodium salt of **L**″ (4-(4′-aminophenylazo)-benzenesulfonic acid) was purchased from Lancaster. Calcium salts were prepared from the sodium salts by reaction with excess $CaCl_2$ in hot water and the acids of **L** and **L**′ were formed by reacting an aqueous solution of the appropriate sodium salt with an excess of concentrated hydrochloric acid. All compounds were reproducibly isolated in near quantitative yields. Crystals of seven compounds were successfully grown to a quality suitable for single crystal analysis using either synchrotron radiation[12] or conventional laboratory techniques. These were found to have the empirical formulas $[Na\{(O_3SC_6H_4)NN(C_6H_4OH)\}(OH_2)_2]$ (**NaL**), $[Ca\{(O_3SC_6H_4)NN(C_6H_4OH)\}_2(OH_2)_2]\cdot 2H_2O$ (**CaL**$_2$), $[(O_3SC_6H_4)N(H)N(C_6H_4OH)]$ (**HL**), $[Na\{(O_3SC_6H_4)NN(C_6H_3(OH)_2)\}(OH_2)_{2.5}]$ (**NaL**′, also known as Tropaelin O or Acid orange 6, CI 14270), $[(O_3SC_6H_4)N(H)N(C_6H_3(OH)_2)]$ (**HL**′), $[Na\{(O_3SC_6H_4)NN(C_6H_4NH_2)\}(OH_2)_2]$ (**NaL**″) and $[Ca\{(O_3SC_6H_4)NN(C_6H_4NH_2)\}_2(OH_2)_4]$ (**CaL**″$_2$). Different batches of these materials were checked for polymorphism primarily by DSC and infra-red spectroscopy. No other polymorphs were observed, except for dehydrated forms of the metal complexes produced as amorphous powders by heating to 95 °C for 12 hours.

Structural descriptions of NaL, CaL$_2$ and HL

NaL was crystallised from both ethanol and water solutions. As expected the yellow-orange plates formed were found to consist of polymeric arrays. Each Na centre has a distorted *fac* octahedral geometry and forms three bonds to water ligands (one terminal and two bridging) and three bonds to O atoms from sulfonate groups. Each pair of neighbouring Na atoms is linked by three bridges (Fig. 1). One link is *via* a bridging water ligand (Na1–O1W = 2.436(2), Na1–O1W* = 2.386(2) Å), one is *via* a single atom bridge provided by the sulfonate (Na1–O1 = 2.400(2), Na1–O1** = 2.356(2) Å) and the last utilises a three atom O–S–O bridge (*via* the three coordinate O1 atom and O2, Na1–O2* = 2.382(2) Å where * is the symmetry operation $1.5 - x$, $0.5 + y$, z and ** is $1.5 - x$, $-0.5 + y$, z). Thus each Na atom is part of six ring systems (two four-membered and four six-membered) linking it to both its nearest neighbouring Na atoms. This cage-like polymeric array propagates along the *b* direction utilising metal–ligand bridges. Each such chain can be viewed in cross-section as a rough rectangle, with only one azo ligand bearing side. The opposite side of the rectangle bears only water ligands, which form hydrogen-bonds to the phenol tails of the azo ligands of a neighbouring chain and thus link the chains in the *c* direction. The structure also propagates in the *a* direction by means of strong hydrogen-bonding between water ligands and sulfonate groups (Fig. 2). Hydrogen-bond details are given in Table 1. The aromatic rings

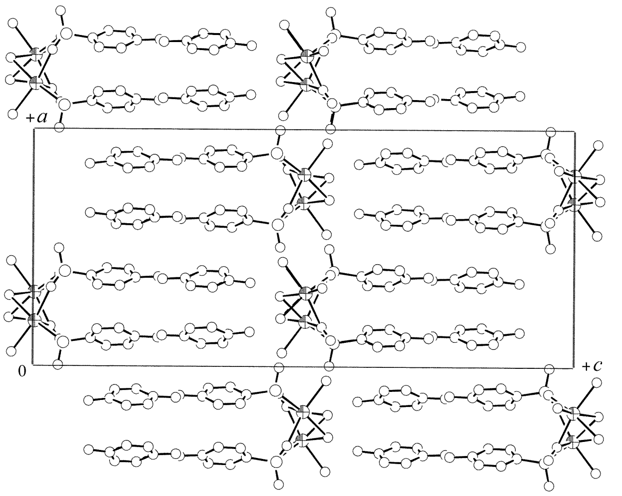

Fig. 2 Extended structure of **NaL** viewed along the *b* axis and hence along the length of the inorganic chains.

Table 1 Hydrogen-bonding in the sodium and calcium complexes, (Å) and (°)

D–H···A	D–H	H···A	D···A	D–H···A
NaL				
O4–H4···O2W	0.83	1.81	2.630	167
O1W–H2W···O4	0.90	2.09	2.895	148
O2W–H3W···O2	0.82	2.03	2.837	166
O2W–H4W···O3	0.80	1.93	2.718	169
NaL′				
O4–H4···O2W	0.76	1.89	2.631	163
O5–H5···N1	0.86	1.74	2.548	156
O2W–H3W···O3W	1.02	1.74	2.734	165
O3W–H5W···O4	0.92	1.84	2.729	161
O3W–H6W···O1	0.86	1.94	2.768	164
NaL″				
O1W–H2W···O3	0.85	2.03	2.862	167
O2W–H3W···O3	0.76	2.12	2.817	151
O2W–H4W···O2	0.94	2.14	2.937	142
N3–H1N···O3	0.97	2.18	3.097	157
CaL$_2$				
O4–H1A···O3W	0.84	1.84	2.637	158
O8–H2A···O4W	0.86	1.76	2.617	172
O1W–H1W···O8	0.85	1.89	2.728	169
O2W–H3W···O4	0.85	1.95	2.788	168
O2W–H4W···O4W	0.78	2.01	2.787	171
O3W–H6W···O3	0.81	2.13	2.910	160
O4W–H7W···O7	0.78	1.97	2.722	160
O4W–H8W···O3W	0.79	2.06	2.825	164
CaL″$_2$				
O1W–H1W···O5	0.79	2.06	2.834	163
O1W–H2W···N3	0.79	2.14	2.926	171
O2W–H3W···O5	1.00	1.93	2.820	146
O3W–H5W···O6	0.86	1.87	2.727	172
O3W–H6W···O3	0.84	2.05	2.869	162
O4W–H8···N6	0.81	2.05	2.851	167

The label W indicates an atom from a water molecule. The maximum standard uncertainties are, for a distance involving a H atom, 0.04 for a distance between non-H atoms, 0.005 Å and for an angle, 3°.

Table 2 Comparison of selected geometric parameters (Å) and (°)

Compound	N1=N2	C4–N1	N2–C7	C4–N1–N2	N1–N2–C7	ω
NaL	1.253(2)	1.430(2)	1.418(2)	113.0(2)	114.8(2)	1.56(8)
CaL$_2$	1.254(4)	1.429(4)	1.427(4)	113.3(3)	114.2(3)	3.9(2)
—	1.250(4)	1.432(4)	1.416(4)	112.4(3)	115.0(3)	4.3(1)
HL	1.269(2)	1.413(2)	1.369(2)	120.2(1)	119.6(1)	24.01(7)
NaL′	1.281(4)	1.414(5)	1.392(4)	114.2(3)	114.2(3)	5.8(2)
HL′	1.278(2)	1.412(2)	1.354(2)	120.9(2)	120.0(2)	2.1(1)
NaL″	1.249(3)	1.424(4)	1.419(3)	113.4(2)	114.7(2)	9.1(2)
CaL″$_2$	1.250(5)	1.424(5)	1.415(5)	113.6(3)	114.7(3)	3.9(3)
—	1.264(5)	1.425(5)	1.415(5)	114.1(4)	113.4(3)	3.7(3)

ω = Dihedral angle between the least-squares planes defined by the six carbon atoms of each aryl ring.

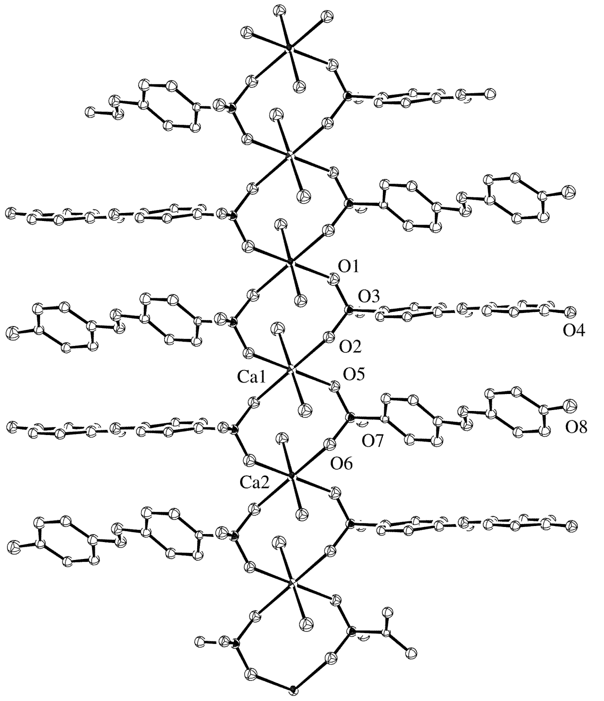

Fig. 3 Extended chain of **CaL$_2$** showing the linked eight-membered rings. Selected bond lengths (Å); Ca1–O2 2.305(2), Ca1–O5 2.336(2), Ca1–O1W 2.338(2), Ca2–O1* 2.328(2), Ca2–O6 2.325(2), Ca2–O2W 2.345(2) where * denotes $-x$, $-y+1$, $-z+1$.

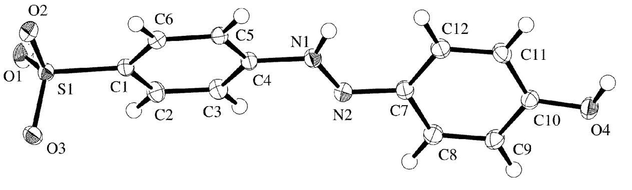

Fig. 4 Molecular structure of **HL**.

are stacked both in the *a* and *b* directions (the closest contacts lie in the *a* direction, C4 · · · C12 3.35, N · · · N 3.77 Å, the closest contact in the *b* direction is C6 · · · C10 3.57 Å). Note that neither the phenol nor the azo groups bond to sodium and that only two of the three O atoms of the sulfonate group do so. O1 is the only three coordinate O atom found in any of the compounds in this study. The N1–N2 bond length of 1.253(2) Å is typical of an azo double bond[13] and the other bond distances are unexceptional. The angle between the planes of the two aromatic rings is 1.56° but the rings are only parallel and not quite coplanar as is shown by the torsion angles N2–N1–C4–C3 and N1–N2–C7–C12 (16.2(3) and −14.8(3)° respectively) which indicate that the azo linkage acts as a step separating the two planes.

Fragile yellow plates of **CaL$_2$** were grown from aqueous solution and after several attempts a crystal of suitable quality for analysis was found. The molecular structures of the azo ligands in **CaL$_2$** were found to be very similar to that in **NaL**, as can be seen from the distances and angles given (Table 2, Fig. 3). Once again the bonding about the metal centre is octahedral but differences in the bridging behaviour of the ligands leads to a very different extended structure. As can be seen, each Ca atom bonds to two terminal and mutually *trans* water ligands. The remaining four bonds are to the O atoms of the sulfonate groups of four azo ligands which form bridges of the M–O–S–O–M type to give a one-dimensional chain of eight-membered rings lying parallel to the *b* direction. This is in marked contrast to the cage arrangement found around the Na atoms in **NaL**. These chains are linked in the *c* direction by hydrogen-bonding interactions between the azos' phenol tails and the water ligands to form sheets perpendicular to the *a* axis. For details of these and other close hydrogen contacts see Table 1. The channels between the sheets contain waters of crystallisation (the only waters not bound to metal found in any of the structures discussed herein). The closest C · · · C contacts across the channels are C22 · · · C6 (3.40 Å) and C16 · · · C8 (3.54 Å).

From visual inspection it is obvious that the free acid of **L** is a different colour from the metal salts of **L** (in aqueous solution λ_{max} of **HL** is 466 nm compared to 353 nm for **NaL** and **CaL$_2$**). To investigate whether or not this colour contrast would correspond to structural changes, red crystals of **HL** were grown from an ethanol solution. It is apparent (Fig. 4) that the proton does not lie on the sulfonate group but on N1. This leads to a number of changes in the chromogen. The N1–N2 bond is lengthened to 1.269(2) Å and both the C4–N1 and especially the N2–C7 bonds are shortened (1.413(2) and 1.369(2) Å respectively). Similar distances were found in the 3,5-dimethylated analogue.[14] The effect of a second resonance structure (Scheme 2) is further shown by the marked pattern of long and short C–C bonds found in the phenol ring (Table 3) which suggest a considerable quinonoid contribution to the overall structure. This supports the conclusions of earlier work[9] based on solid-state ^{13}C and ^{15}N NMR which showed an enhanced positive charge at C10.

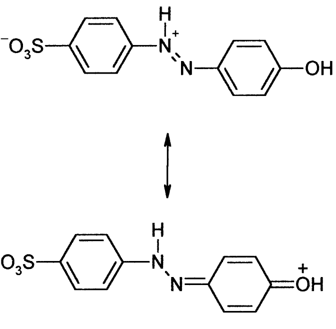

Scheme 2

The sulfonate bearing ring does not contribute so markedly to this resonance stabilisation and is twisted considerably out of plane (dihedral angle between the planes of the aromatic rings is 24.01(7)°). This twist is possibly influenced by the formation of an intermolecular hydrogen-bond between the proton of N1 and O2, Table 4. A final effect of the protonation of the azo is that both the angles N1–N2–C7 and N2–N1–C4 now have values very close to that for idealised sp^2 geometry (119.6(1) and 120.1(1)° respectively). The equivalent angles for the five metal containing structures presented here all have compressed values in the range 113.0(1) to 115.0(3)°, presumably due to an increased steric contribution from the azo lone pairs.

Solid-state Raman spectroscopy emphasises the similar nature of the azo centred chromophore in **NaL** and **CaL$_2$** as both give bands which can be attributed to the N–N stretch at 1440 cm^{-1}. **HL** is different and the N–N bond has more single bond character as confirmed by its frequency of 1370 cm^{-1}. The Raman data thus agrees with the molecular structures determined by X-ray diffraction. Solid-state uv/vis reflectance spectra were also measured. As noted above both the metal complexes of **L** give similar solution spectra (as does **HL** at higher pHs). **NaL** and **CaL$_2$** both give hypsochromic shifts on crystallisation but do so to different degrees (λ_{max} = 345 and 318 nm respectively). As the molecular geometry of the azo ligand in each is similar, as measured by single crystal diffraction and by Raman spectroscopy, it seems reasonable to infer that the difference in colour is due to the different inter- and supra-molecular interactions present. In contrast, **HL** in the solid-state absorbs at a longer wavelength (503 nm, a bathochromatic shift) than in aqueous solution.

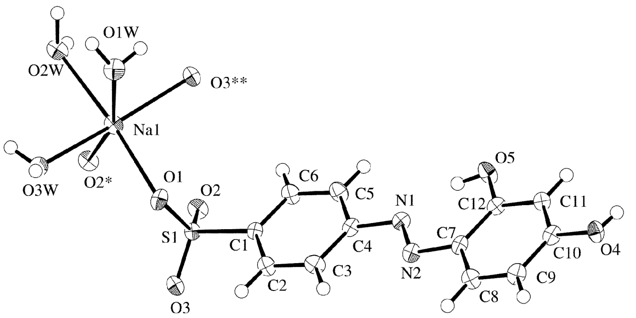

Fig. 5 The molecular structure of **NaL′**. Selected bond lengths (Å); Na1–O2* 2.349(3), Na1–O3W 2.370(3), Na1–O3** 2.387(3), Na1–O1W 2.449(3), Na1–O1 2.466(3), Na1–O2W 2.595(3) where * denotes $-x, -y, -z + 1$ and ** is $x, y - 1, z$.

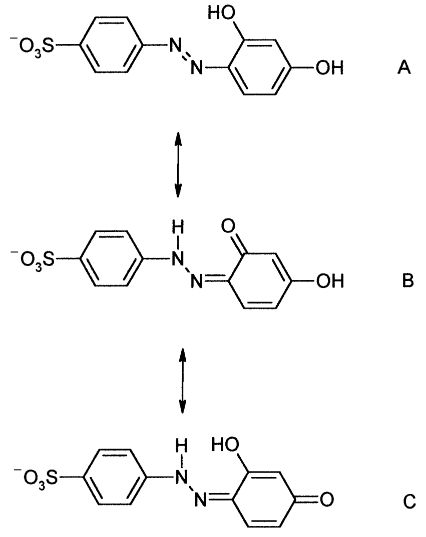

Scheme 3

Structural descriptions of NaL′ and HL′

L′ was designed with a hydroxy substituent *ortho* to the azo both to provide an extra possible metal binding or hydrogen-bonding site and also to provide the possibility of tautomerism to the keto-hydrazone (Scheme 3) as is found in commercial monoazo pigments such as Ca4B.[4] However, the diffraction study on an orange needle of **NaL′** unequivocally shows the proton to be bonded to O and not to N, Fig. 5. (An attempt to model a disordered proton position over two sites with a sum occupancy of one gave an occupancy of 0 to the hydrazo site and 1 to the hydroxyl site.) Despite this the bond lengths do show a lengthening of the N1–N2 bond (1.281(4) Å) and a shortening of the C4–N1 and N2–C7 bonds (1.414(5) and 1.392(4) Å respectively). The azo bond is thus longer than the protonated azo bond of **HL** but is still shorter than that found in the keto-hydrazone pigment of ref. 4 (1.304(2) Å). The C–C and N–C bonds are however not as distorted as in **HL**, although the C7–C12 distance of 1.413(5) Å indicates considerable single bond character. The azo ligand is planar (N1–N2–C7–C12 0.3(5) and N2–N1–C4–C3 −1.1(5)°) stabilised in part by the formation of a six-membered ring *via* intramolecular hydrogen-bonding (O5 · · · N1 2.548(4) Å, Table 1).

Table 3 Selected distances; effect of resonance contributions to bond lengths (Å)

	NaL	NaL′	HL	HL′
N1=N2	1.253(2)	1.281(4)	1.269(2)	1.278(2)
N2–C7	1.418(3)	1.392(4)	1.369(2)	1.354(2)
C7–C8	1.390(3)	1.405(5)	1.407(2)	1.426(3)
C8–C9	1.385(3)	1.365(5)	1.370(2)	1.363(3)
C9–C10	1.388(3)	1.394(5)	1.401(2)	1.424(3)
C10–C11	1.395(3)	1.385(5)	1.413(2)	1.387(3)
C11–C12	1.385(3)	1.381(5)	1.368(2)	1.392(3)
C12–C7	1.398(3)	1.413(5)	1.413(2)	1.430(3)
C10–O4	1.367(2)	1.353(4)	1.330(2)	1.332(2)
C12–O5		1.343(4)		1.330(3)

As in **NaL** the Na atom is at the centre of a distorted octahedral arrangement of O atoms, three from water ligands and three from sulfonate groups in a *fac* arrangement. However, once again differing ligand bridging modes lead to a different three-dimensional structure. Each sulfonate uses all three of its oxygen atoms to bond to Na and all three contribute to M–O–S–O–M bridges. This gives a series of interlocked eight-membered [$Na_2S_2O_4$] rings that propagate a double chain of Na atoms along the *b* direction, Fig. 6. One of the water ligands also acts in a bridging mode and links the chains of 8-

Table 4 Hydrogen-bonding interactions in the free acids **HL** and **HL′**, (Å) and (°)

D–H · · · A	D–H	H · · · A	D · · · A	D–H · · · A	Symmetry operation
HL					
N1–H1 · · · O2	0.92(2)	1.94(2)	2.801(2)	154(2)	$x + 0.5, -y + 0.5, z + 0.5$
O4–H4 · · · O3	0.87(2)	1.77(2)	2.632(2)	173(1)	$x + 1, y, z + 1$
HL′					
O5–H5H · · · N2	0.87(3)	2.30(3)	2.715(2)	109(2)	
N1–H1N · · · O3	0.89(3)	2.06(3)	2.857(2)	147(2)	$x, -y - 0.5, z - 0.5$
O4–H4H · · · O1	0.89(3)	1.78(3)	2.668(2)	173(2)	$x, y, z - 1$
O5–H5H · · · O2	0.87(3)	2.03(3)	2.760(2)	140(2)	$-x + 1, -y, -z + 2$

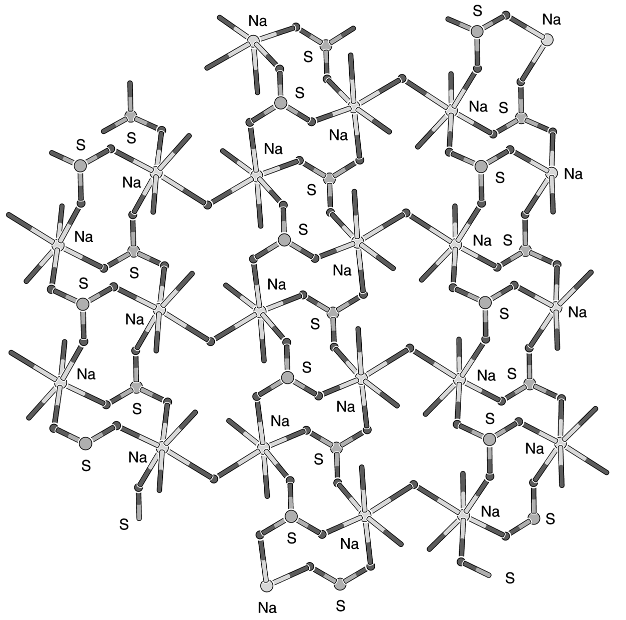

Fig. 6 Part of the inorganic coordination net of **NaL**′, showing the interlocking 8- and 12-membered rings. Each ring has contributions from two sulfonates with mutually *anti* azos.

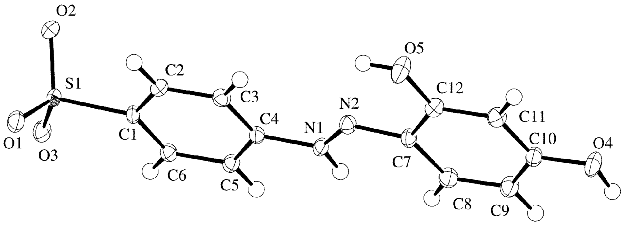

Fig. 7 Molecular structure of **HL**′.

membered rings, *via* 12-membered rings, into sheets parallel to the *ab* plane. The polymeric net formed utilises each S-atom as a three way junction and each Na-atom as a four way junction. All the rings, whether 8- or 12-membered, contain two mutually *anti* sulfonate/azo ligands. These inorganic sheets are then linked by the azo ligands *via* hydrogen bonds involving the azo's phenol tail. There are several contacts short enough to be considered as π–π interactions, involving both the aromatic rings and the azo group (shortest contacts C4 · · · C12 3.36, C5 · · · C12 3.53, C6 · · · C10 3.57, N2 · · · C8 3.49, C12 · · · N1 3.50 and N1 · · · N1 3.60 Å). This is a different array from all the other examples discussed so far. **NaL** and **CaL$_2$** form metal to ligand coordination bonds that combine to give one-dimensional chains of rings or cages from which three-dimensional structures are built by hydrogen-bonding and π-stacking. By contrast, **NaL**′ forms a two-dimensional sheet utilising coordinated metal to ligand bonds.

On growth from an ethanol solution, the free acid of **L**′ formed red, tabular crystals. As with **HL**, **HL**′ exists as the azonium tautomer with protonation at N1. This protonation breaks the internal, 6-membered hydrogen-bond found in **NaL**′ and results in the C7 to C12 ring rotating 180° about the N2–C7 bond (Fig. 7). Despite the breaking of the internal hydrogen-bonding, and in contrast to **HL**, the azo ligand remains essentially planar (dihedral angle between the planes of the aryl rings is 2.1(1)°). Although there is now a weak intramolecular contact between the hydroxy group of O5 and N2, which should favour retention of overall planarity, the intermolecular hydrogen-bonds from both OH groups and from the proton on N1 to the three O atoms of the sulfonate group are all significantly shorter and stronger (Table 4).

The C–C distances of the OH bearing ring clearly show the pattern of long and short bonds (Table 3) associated with the resonance form B shown in Scheme 3. This distortion is more marked than in **NaL**′, a point further emphasised by the relative C–O distances. Despite this the N1–N2 distances of the two species are identical (1.278(2) and 1.281(4) Å for **HL**′ and **NaL**′) indicating the elongating effect of the short intramolecular hydrogen bond in **NaL**′.

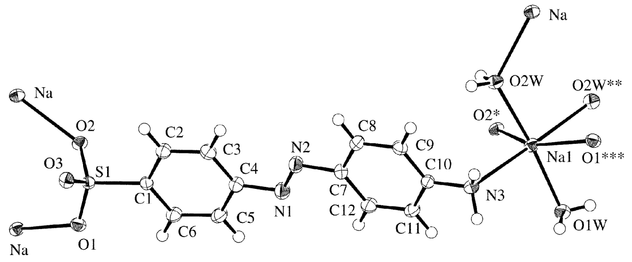

Fig. 8 The molecular structure of **NaL**″. Selected bond lengths (Å); Na1–O2* 2.353(2), Na1–O2W 2.365(3), Na1–O1W 2.365(3), Na1–O2W** 2.441(2), Na1–N3 2.525(3), Na1–O1*** 2.541(2) where * is $-x, y - 0.5, -z - 1$, ** is $-x, y - 0.5, -z$ and *** is $x, y, z + 1$.

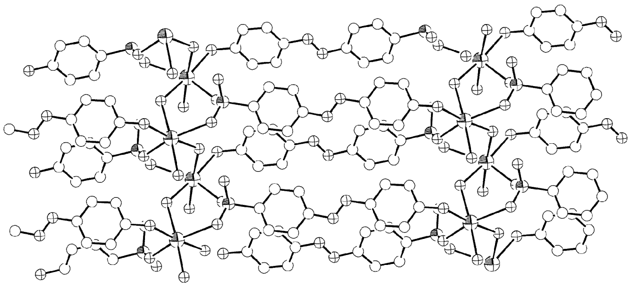

Fig. 9 Expanded structure of **NaL**″ viewed along the *a* direction.

Structural description of NaL″ and CaL″$_2$

High quality crystals of **NaL**″ were easily grown as yellow-orange needles from aqueous solution. Again it was found that a simple change to the azo ligand produced little change to the internal geometry of the ligand (all bond lengths and angles are in good agreement with those found for **NaL** and **CaL$_2$**, Table 2, and also with those found in the related structure of ethanol solvated methyl orange).[15] However, a different polymeric array was formed. The coordination geometry about the Na atom is octahedral but in this case with bonds to three *mer* water ligands, two mutually *trans* O atoms from sulfonate groups and the N atom of the ligands amine tail. Each set of neighbouring Na atoms is linked by one bridging water ligand and one M–O–S–O–M type bridging sulfonate to form a chain of six-membered rings that propagates about the 2$_1$ axis and hence the *b* direction, Figs. 8 and 9. This is reminiscent of the chains of eight-membered rings found in **CaL$_2$**. **L**″ is the only one of the three ligands herein to use its tail to adopt a genuinely bidentate bonding mode with Na–N3 = 2.525(3) Å closely matching related distances in the literature.[16]

The hydroxy tails of **L** and **L**′ are involved solely in hydrogen-bonding and the sterically hindered dimethylamine tail of methyl orange forms no intermolecular contact at all.[15] The inorganic chains are thus linked by the azo ligands to form a sheet structure perpendicular to the *a* axis. Hydrogen-bond details are given in Table 1. These appear weaker than in the other compounds. Similarly, the role of ring stacking in the **NaL**″ structure appears to be less important than in the previously discussed structures, with fewer (and longer) close contacts (only C6 · · · C10 = 3.54 Å is within the distance usually regarded as significant). This may be because the azo ligands are now firmly held at both ends, thus limiting their degree of freedom to adopt D–H · · · A or π–π bonding conformations, whereas the metal salts of **L** and **L**′ form relatively

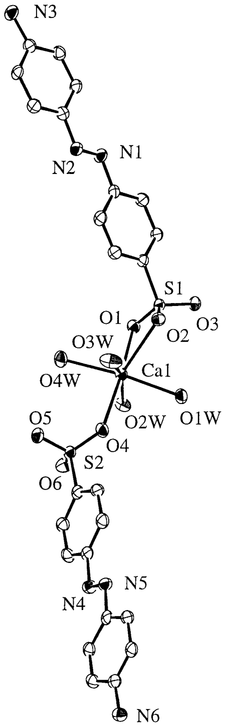

Fig. 10 The molecular structure of **CaL″**$_2$. Selected bond lengths (Å); Ca1–O4 2.325(3), Ca1–O3W 2.333(3), Ca1–O1W 2.376(3), Ca1–O2W 2.383(3), Ca1–O4W 2.389(3), Ca1–O2 2.504(3), Ca1–O1 2.508(3).

conformationally-flexible hydrogen-bonds with their phenol tails. This is supported by the observation that in the structure of **CaL″**$_2$, which has no bridging ligands of any type, there is extensive π–π stacking between anti-parallel pairs of azo ligands (shortest contact N5 · · · C24 3.33 Å). Thus it is not the integral nature of **L″** that lessens the hydrogen-bonding and π–π contacts in **NaL″** but the suprastructural environment in which it is situated. The structure of **CaL″**$_2$ is once again different from all the preceding structures, containing no polymeric array forming coordination bonds (the three-dimensional structure is completed by extensive hydrogen-bonding involving the amine, water and sulfonate groups, see Table 1).

The structure is interesting (Fig. 10) as the two crystallographically independent azo ligands bond in manners not observed previously for **L**, **L′** or **L″**. **NaL′** displayed a bridging η^3 bonding mode for the sulfonate, and the other structures all involve the sulfonate in η^2 modes with a variety of bridge types. **CaL″**$_2$ has one η^1 bonded sulfonate and one η^2 bonded sulfonate where both O atoms are bound to the same metal site. The Ca to O bond length of the η^1 bonded sulfonate lies within the range found for the η^2 bonded sulfonates (Ca1–O4 2.325(3) Å for **CaL″**$_2$ compared to 2.305(2) to 2.336(2) Å for **CaL**$_2$), but the values found for Ca1–O1 and Ca1–O2 are much longer (2.508(3) and 2.504(3) Å). The geometric parameters for the **L″** ligands are similar to those found in **NaL**, **CaL**$_2$ and **NaL″**, with the exception of the azo bond length of the η^1 sulfonate ligand which is longer than typical (N4–N5 1.264(5)). This may indicate a change in chromophore associated with the η^1 sulfonate bonding mode, but it should be noted that evidence for this is weakened as the ligand does not show the other bonding distortions seen in **HL** and **NaL′** and that the structural determination of **CaL″**$_2$ is of lower quality than the preceding structures.

Conclusions

This study has described five different three-dimensional arrays formed by sulfonated monoazo ligands with sodium or calcium. The structure of a calcium azo laked pigment[4] and of a methyl orange solvate are also known from the literature.[15] It is apparent that even with these simple systems there is an extreme variety of regular, well formed structural motifs which are controlled by the groups on the parent azo dyes. For example, for these seven s-block metal complexes of closely related ligands we observe sulfonate groups that can form η^1, η^2 or η^3 interactions with the metal. If they are η^2 bound, they can interact with two metal atoms or just one and they can, if bridging, bridge in one or both of two different ways. Additionally, the water molecules are free, terminally bound or bridging and all the polymeric arrays observed are different from one another. The effects these variables, either singly or in combination, could have on colour and other physical properties are currently unknown. However, it is now possible to make some generalisations concerning the arrays formed, based on the available data.

The inorganic architecture of the structures dominates the organic bonding motifs. That is to say that the coordination bonds involving the metals, the sulfonate groups and the water ligands appear to form polymeric assemblies with the azo ligands at their peripheries. The inter-organic hydrogen-bonds and π–π interactions are maximised using whatever flexibility is left to the azo ligands. This is illustrated by the minimisation of inter-organic interactions in the least flexible inorganic architectures (*e.g.* the sheets of **NaL″**) and also rather nicely by Fig. 3 where it can be seen that [CaOSO]$_2$ rings are too widely spread to allow parallel π–π stacking of the rings of **L**. If the π–π interaction was dominant then it would be expected that another inorganic motif could be utilised, perhaps involving smaller six-membered rings and a differing metal bridging mode. However, the organic building blocks do influence the inorganic structure. This is amply demonstrated by the range of different structures produced herein merely by changing one substituent on an aryl ring. A second general point (when considering only the coordinatively bound motifs) is the Na species adoption of traditional inorganic "mineral-like" motifs of closely linked sheets, chains and cages. This is in contrast to the more open, simpler chain and monomer based structures of the Ca species, reminiscent of the ring ladders found throughout s-block amide chemistry.[17] The difference is caused by the higher ratio of ligand to metal for the dicationic metal. Several specific points can be added to these general observations. None of the calcium structures utilise bridging water ligands whilst all the sodium structures do so. Again this may be related to the higher ratio of azo ligands present. With the exception of the chelate species of ref. 4, all the metal centres bond to six ligands in octahedral or pseudo-octahedral arrangements. Coordination to sodium or calcium does not alter the bond lengths or angles of the ligands away from the norm expected for simple azos and typical nitrogen to nitrogen double bond lengths are found throughout. However, both protonation of the ligand and the presence of tautomerisable groups have readily understandable effects on the molecular structure of the conjugated system. All the azo ligands herein adopt planar conformations when bound to a metal. This is not a trivial observation, as twisted conformations are found both for the DL-lysine salt of **L**[8] and for **HL**.

Finally, and in contrast to the transition metal chemistry of azos,[18] none of the azo nitrogen atoms are involved with bonding to metals and perhaps more surprisingly neither are any of the hydroxyl groups. In contrast the NH$_2$ tail of **L″** does bond to sodium. This is counter intuitive since most sodium and calcium compounds form strong metal to oxygen bonds (as an illustration of this see the much greater number of M(ROH) compounds to be found in the CCSD as opposed to M(RNH$_2$) compounds).[5] Furthermore, despite the largely ionic nature of Na bonds, the amine does not displace a water ligand from the coordination shell of Na but in fact reduces the number of sulfonate contacts (as compared to **NaL** and **NaL′**).

Table 5 Crystallographic data and refinement parameters

	NaL	**CaL$_2$**	**HL**	**NaL′**	**HL′**	**NaL″**	**CaL″$_2$**
Formula	$C_{12}H_{13}N_2NaO_6S$	$C_{24}H_{26}CaN_4O_{12}S_2$	$C_{12}H_{10}N_2O_4S$	$C_{12}H_{14}N_2NaO_{7.5}S$	$C_{12}H_{10}N_2O_5S$	$C_{12}H_{14}N_3NaO_5S$	$C_{24}H_{24}CaN_6O_8S_2$
Mol. wt.	336.29	666.69	278.28	361.30	294.28	335.31	628.69
System	Orthorhombic	Triclinic	Monoclinic	Monoclinic	Monoclinic	Monoclinic	Monoclinic
a/Å	14.383(1)	9.0921(4)	9.6753(4)	35.036(9)	8.3957(2)	7.829(3)	8.147(5)
b/Å	5.8131(4)	9.9442(4)	10.6210(5)	5.410(2)	10.0367(2)	5.784(5)	32.892(12)
c/Å	32.891(2)	16.4920(6)	11.6835(5)	15.978(4)	14.0101(3)	16.486(3)	10.553(4)
α/°		99.235(2)					
β/°		97.684(2)	99.346(2)	98.050(7)	99.996(2)	98.62(2)	91.77(4)
γ/°		104.208(2)					
U/Å^3	2750.0(3)	1403.2(1)	1184.68(9)	2998.9(14)	1162.64(4)	738.1(5)	2826(2)
T/K	150	150	150	150	150	173	123
λ/Å	0.6891	0.71073	0.6891	0.6891	0.71073	0.71069	0.71069
Space group	$Pbcn$	$P\bar{1}$	$P2_1/n$	$C2/c$	$P2_1/c$	$P2_1$	$P2_1/n$
Z	8	2	4	8	4	2	4
μ/mm^{-1}	0.299	0.444	0.285	0.287	0.302	0.275	0.427
2θmax/°	54	55	55	50	54	55	50
Refl. measured	16505	11255	7543	7726	19332	3938	5333
Refl. unique	3282	6330	2906	2901	2557	3341	4967
R_{int}	0.0337	0.0459	0.0311	0.0665	0.056	0.0242	0.1074
$R1$	0.0417	0.0545	0.0374	0.0633	0.0403	0.0436	0.0735
$wR2$	0.0902	0.1492	0.1038	0.1568	0.0949	0.1113	0.2190
Refl. observed	2900	4659	2638	2210	2037	3147	3985
Parameters	219	446	180	241	193	222	436
GoF	1.215	1.090	1.060	1.082	1.036	1.040	1.027

Rational pigment and ink-jet dye design depends upon correlating solid-state structure to physical properties. However, control of the solid-state structure of molecular materials is frustrated both by complexity and by a lack of directionality in intermolecular forces.[19] Here we have begun to assess a previously neglected supramolecular system which though complex does appear to possess regularity and structure. The elucidation of the structures reported herein provides the necessary first step towards understanding solid-state, dye–dye interactions in sulfonated monoazo colourants.

Experimental

Raman spectra were recorded on a Renishaw System RM 2000. Excitation, at 785 nm, was provided by a diode laser. Solid-state uv/vis spectra were recorded on a Phillips PU8740 spectrophotometer in reflectance mode and aqueous solution spectra were recorded on the same machine in transmission mode. DSC measurements were made with a DuPont 910 DSC equipped with a DuPont 990 program and recorder.

Single crystal diffraction data were recorded by a Rigaku AFC7S diffractometer for **NaL″** and **CaL″**$_2$, by a Nonius Kappa CCD for **CaL**$_2$ and **HL′** and at Station 9.8 of the Daresbury Synchrotron Radiation Source for **NaL**, **HL** and **NaL′**. All non-H atoms were refined anisotropically and the H atoms bonded to O or N were refined isotropically. All other H atoms were placed in calculated positions and in riding modes. The structures were refined against F^2 to convergence using the SHELXL-97 program.[20] Specific crystallographic data and refinement parameters are given in Table 5.

CCDC reference numbers 161656–161662.

See http://www.rsc.org/suppdata/dt/b1/b102106k/ for crystallographic data in CIF or other electronic format.

Acknowledgements

M. P. H. acknowledges the help of G. Dent of Avecia and the receipt of a CASE studentship from Avecia and the EPSRC.

References

1 See for example: A. J. Blake, N. R. Champness, P. Huberstey, W.-S. Li, M. A. Withersby and M. Schröder, *Coord. Chem. Rev.*, 1999, **183**, 117; M. J. Plater, M. R. St. J. Foreman, T. Gelbrich, S. J. Coles and M. B. Hursthouse, *J. Chem. Soc.*, *Dalton Trans.*, 2000, 3065; P. J. Strang and B. Olenyuk, *Acc. Chem. Res.*, 1997, **30**, 502; S.-P. Yang, X.-M. Chen and L.-N. Ji, *J. Chem. Soc.*, *Dalton Trans.*, 2000, 2337.

2 H. Bock, J.-M. Lehn, J. Pauls, S. Holl and V. Krenzel, *Angew. Chem.*, *Int. Ed.*, 1999, **38**, 952; L. Zhang, P. Cheng, L.-F. Tang, L.-H. Weng, Z.-H. Jiang, D.-Z. Liao, S.-P. Yan and G.-L. Wang, *Chem. Commun.*, 2000, 717; W. S. Sheldrick, *J. Chem. Soc.*, *Dalton Trans.*, 2000, 3041.

3 Z. Hao and A. Iqbal, *Chem. Soc. Rev.*, 1997, **26**, 203.

4 A. R. Kennedy, C. McNair, W. E. Smith, G. Chisholm and S. J. Teat, *Angew. Chem.*, *Int. Ed.*, 2000, **39**, 638.

5 F. H. Allen and O. Kennard, *Chem. Des. Autom. News*, 1993, **8**, 31.

6 For a notable exception see: C. C. Evans, L. Sukavto and M. D. Ward, *J. Am. Chem. Soc.*, 1999, **121**, 320.

7 P. Gregory, *Chem. Brit.*, 2000, **36–8**, 39.

8 W. H. Ojala, E. A. Sudbeck, L. K. Lu, T. I. Richardson, R. E. Lovrien and W. B. Gleason, *J. Am. Chem. Soc.*, 1996, **118**, 2131.

9 A. M. Chippendale, G. McGeorge, R. K. Harris and C. M. Brennan, *Magn. Reson. Chem.*, 1999, **37**, 232.

10 Y. Saito, B.-K. Kim, K. Machida and T. Uno, *Bull. Chem. Soc. Jpn.*, 1974, **47**, 2111; P. Savarino, G. Viscardi, E. Barni, R. Carpignano and A. L. Federov, *Dyes Pigm.*, 1990, **13**, 71.

11 L. R. Whitlock, S. Siggia and J. E. Smola, *Anal. Chem.*, 1972, **44**, 532.

12 R. J. Cernik, W. Clegg, C. R. A. Catlow, G. Bushnell Wye, J. V. Flaherty, G. W. Greaves, I. Burrows, D. J. Taylor, S. J. Teat and M. Hamichi, *J. Synchrotron Radiat.*, 1997, **4**, 279.

13 For a typical example see: A. Crispini, M. Ghedini and D. Pucci, *Acta Crystallogr.*, *Sect. C*, 1998, **54**, 1869.

14 N. Ehlinger and M. Perrin, *Acta Crystallogr.*, *Sect. C*, 1995, **51**, 1846.

15 A. W. Hanson, *Acta Crystallogr.*, *Sect. B*, 1973, **29**, 454.

16 J. W. Swardstrom, L. A. Duvall and D. P. Miller, *Acta Crystallogr.*, *Sect. B*, 1972, **28**, 2510.

17 R. E. Mulvey, *Chem. Soc. Rev.*, 1998, **27**, 339.

18 S. B. Choudhury, D. Ray and A. Chakravorty, *J. Chem. Soc.*, *Dalton Trans.*, 1992, 107.

19 A. Gavezzotti, *Acc. Chem. Res.*, 1994, **27**, 309.

20 G. M. Sheldrick, SHELXL-97, program for crystal structure refinement, University of Göttingen, 1997.